Received: 2 June 2024 | Revised: 22 August 2024 | Accepted: 23 August 2024

DOI: 10.1002/pamm.202400212

RESEARCH ARTICLE

Inductive mode selective damping of structural vibrations

Mitja Rosenboom | **Hartmut Hetzler**

Universität Kassel, Kassel, Germany

Correspondence
Mitja Rosenboom, Universität Kassel, Mönchebergstraße 7, 34125, Kassel, Germany.
Email: rosenboom@uni-kassel.de

Abstract

Structural vibrations pose significant challenges in various engineering applications and require effective damping strategies to improve the overall performance and longevity of systems. While some oscillations can significantly reduce the longevity of systems, others might contribute positively to the overall system performance. Thus, this contribution presents a novel method of an inductive damping concept, that targets only specific vibrational modes based on their mode shapes. By analyzing the used inductive damping element in the context of a single degree of freedom oscillator, it is shown, that it functions as an ideal viscous damper only if the dynamics of the electric part of the system are neglected. The concept of mode selective damping is presented, using two of these damping elements in an oscillator chain with three masses. By altering the wiring configurations connecting the two damping elements in the electrical domain, the damping behavior can be manipulated to selectively damp only specific modes according to their mode shapes.

1 | INTRODUCTION

Reducing resonant amplitudes of machinery and buildings presents a significant challenge in engineering mechanics. In addition to classical fluid dampers, friction dampers, particle dampers and tuned mass dampers, inductive damping methods are a well established concept and have been analyzed by numerous research groups [1–4]. Beside the classical approaches also combinations of different methods have been established, such as magnetorhelogical fluid dampers [5] or recently Alhams et al. [6] investigated a combination of eddy current damping with a conventional automotive hydraulic damper. Since not all vibrations occurring in engineering applications are undesired – some may contribute positively to overall system dynamics, such as enhancing comfort or reducing fundamental forces – damping systems designed to specifically attenuate amplitudes of certain modes offer a potential solution to address this conflict of objectives. One way of realizing such damping systems is to use inductive dampers, where the individual damping elements interconnect with each other. For this purpose, inductive damping elements are preferable, as they can interchange information in the electric domain via wires, that can be readily integrated into systems. To the best of our knowledge, such a system has not been analyzed before. Therefore, the aim of this work is to highlight the concept of the inductive mode selective damping.

This paper begins by establishing a simplified mathematical model for the inductive damping element. The fundamental behavior of this damping element is demonstrated by applying it to a single degree of freedom (DoF) oscillator.

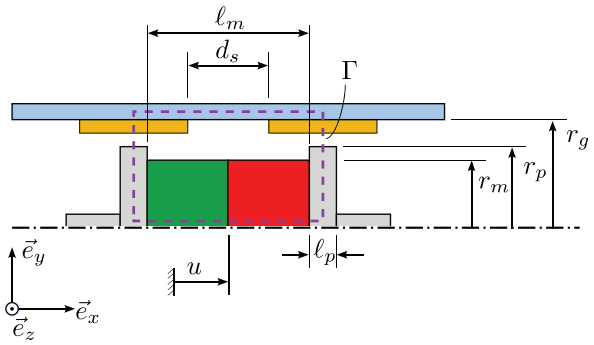

FIGURE 1 Model of the inductive damping element and its components (grey - plunger, green/red - permanent magnet, blue - housing, yellow - coils) with all geometric quantities and the loop Γ (dashed purple line) to calculate the magnetic flux density using AMPÉRE's law.

Subsequently, multiple such elements are integrated into an oscillator chain and various methods of interconnecting these elements are presented and analyzed.

2 | THE INDUCTIVE DAMPING ELEMENT

The inductive damping element under analysis is illustrated in Figure 1 and has been analyzed for example, by Palomera-Arias [1]. It consist of a plunger (grey), with an attached permanent magnet (green/red), moving inside a housing (blue) containing two coils (yellow). The relative motion between the permanent magnet and the coils induces an electromotive force in the coils. Closing the electric circuit of the coils induces a current, leading to the conversion of energy into heat due to the ohmic resistance of the coils or additional resistors, and thereby dissipating energy from the system.

2.1 | Modeling of the damping element

The derivation of the governing equations of motion will be proceeded by means of LAGRANGE's equations of second kind for electromechanical systems [7]. Therefore the Lagrangian is given by

$$\mathcal{L} = T^* - U + W_m^* - W_e, \tag{1}$$

where T^* is the kinetic co-energy, U is the (mechanical) energy, W_m^* is the magnetic co-energy and W_e is the electric energy. Since no lumped capacities will be included in the model and the capacities of the coils are negligible it is assumed that the the electric energy is negligible, and thus

$$W_e = 0. \tag{2}$$

The main task to include the inductive damping element into the Lagrangian is to calculate the magnetic co-energy. In the proposed damping model this can be expressed as

$$W_m^* = \int \Psi \, \mathrm{d}I, \tag{3}$$

where, Ψ is the flux linkage of the coils and I is the current flowing through the coils. Considering the self inductance as a fixed parameter L, the flux linkage reads

$$\Psi = LI + \sum_{i=1}^{N} \int_{A(i)} B_{x,i} \, \mathrm{d}a, \tag{4}$$

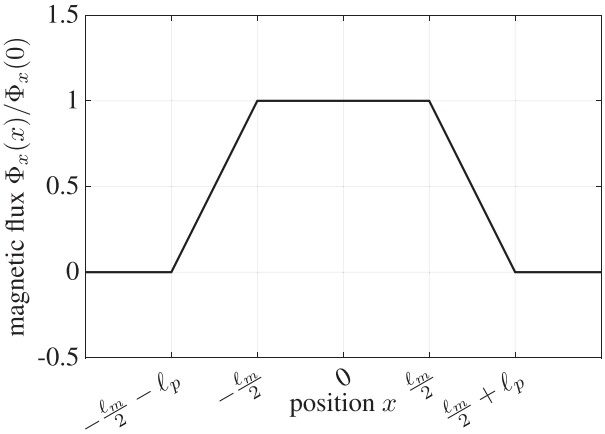

FIGURE 2 Distribution of the relative magnetic flux $\Phi_x(x)/\Phi_x(0)$ through the inside of the housing for a centered plunger.

where $B_{x,i}$ is the magnetic flux density in x-direction at the i-th winding of the coil with cross section A_i and N is the number of turns of the coil. To overcome the sum, a winding density ρ_w is introduced. With this, the flux density can be written as

$$\Psi = LI + \int_{\ell}\int_{A(x)} B_x(x)\,\mathrm{d}a\rho_w\,\mathrm{d}x, \tag{5}$$

where ℓ is the length of the coil. Since all cross sections of the coil are equal this further simplifies to

$$\Psi = LI + A\rho_w \int_{\ell} B_x(x)\,\mathrm{d}x. \tag{6}$$

Thus, it is left, to calculate the magnetic flux density. This can be done by applying AMPÉRE's law to the loop Γ illustrated in Figure 1.

If flux leakage is neglected and it is assumed, that all the flux follows the considered path and is only radially orientated in the airgap – respectively at the coils – and furthermore all iron parts are considered to have infinite permeability,[1] the magnetic flux due to the permanent magnet is given by

$$B_0 = B_r \frac{1}{1 + \frac{r_m^2}{\ell_p \ell_m}(\ln(r_g) - \ln(r_p))}. \tag{7}$$

Herein B_r is the remanent flux of the permanent magnet, r_m is its radius and ℓ_m is its length. Furthermore r_g is the radius of the housing, r_p is the radius of the pole shoes and ℓ_p is the length of the pole shoes. All the geometric quantities are visualized in Figure 1. Assuming a piecewise linear magnetic flux in x-direction in the inside of the coils, as shown in Figure 2, the flux linkage, depending on the displacement u of the plunger, reads

$$\Psi = LI - Ku \quad \text{with} \quad K = 2\pi r_m^2 B_0 \rho_w\,. \tag{8}$$

3 | APPLICATION TO SINGLE DEGREE OF FREEDOM OSCILLATOR

In the following the inductive damping element is analyzed in the context of a single DoF oscillator, as shown in Figure 3. The equations of motion are derived by means of LAGRANGE's equations of second kind for electromechanical systems. A

[1] These simplifications are necessary to keep the size of the model small. Since flux leakage and saturation and so forth. lead to a reduced magnetic flux density, the model overestimates the coupling coefficient K. However, only a qualitative analysis is performed in this work, so the simplified model is sufficient. For quantitative results a more detailed model must be used.

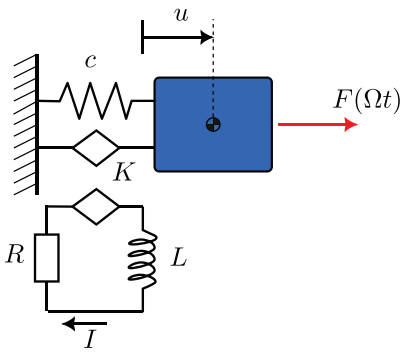

FIGURE 3 Single DoF Oscillator with inductive damping element. DoF, degree of freedom.

parameter reduction is performed and the reduced system is investigated. Finally, the influence of the different parameters is discussed.

3.1 | Derivation of equations of motion for single DoF oscillator

The kinetic co-energy and potential energy of the system are given by

$$T^* = \frac{1}{2}m\dot{u}^2 \quad \text{and} \quad U = \frac{1}{2}cu^2. \tag{9}$$

With the flux linkage derived in the previous section, the magnetic co-energy yields

$$W_m^* = \frac{1}{2}LI^2 - KuI \tag{10}$$

and therefore the Lagrangian is given by

$$\mathcal{L} = \frac{1}{2}m\dot{u}^2 - \frac{1}{2}cu^2 + \frac{1}{2}LI^2 - KuI \tag{11}$$

with the independent variables I and u and the non-conservative forces read

$$Q_I = -RI \quad \text{and} \quad Q_u = F(\Omega t) \tag{12}$$

where R is the ohmic resistance of each coil and $F(\Omega t)$ is a harmonic excitation force. Applying LAGRANGE's equations of second kind and substituting the electric current by the electric charge, that is,

$$I = \frac{\mathrm{d}q}{\mathrm{d}t}, \tag{13}$$

the equations of motion are found as

$$\begin{bmatrix} m & 0 \\ 0 & L \end{bmatrix} \begin{bmatrix} \ddot{u} \\ \ddot{q} \end{bmatrix} + \begin{bmatrix} 0 & K \\ -K & R \end{bmatrix} \begin{bmatrix} \dot{u} \\ \dot{q} \end{bmatrix} + \begin{bmatrix} c & 0 \\ 0 & 0 \end{bmatrix} \begin{bmatrix} u \\ q \end{bmatrix} = \begin{bmatrix} F(\Omega t) \\ 0 \end{bmatrix}. \tag{14}$$

Since this investigation focuses on the conceptional side, the equations of motion are transferred into non-dimensional form. Therefore, the parameters

$$\omega_0 = \sqrt{\frac{c}{m}} \qquad f = \frac{F}{c\ell} \qquad \xi = \frac{u}{\ell}$$

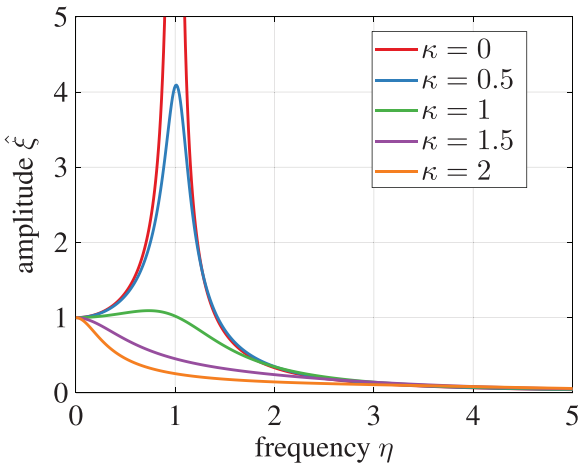

FIGURE 4 Frequency response function of single DoF Oscillator with inductive damping element for different values of κ and a value of $\nu = 0$. DoF, degree of freedom.

$$T_0 = \frac{L}{R} \qquad I_0 = \frac{m\ell^2}{LT_0^2} \qquad \zeta = \frac{q}{T_0 I_0} \tag{15}$$

$$\kappa = \frac{KI_0T_0}{m\ell\omega_0} \qquad \nu = T_0\omega_0 \qquad \tau = \omega_0 t$$

are introduced, where ℓ is some arbitrary reference length. Due to the substitution of the time, derivatives with respect to t are substituted by derivatives with respect to τ, which are denoted by $(\cdot)'$. With this, the non-dimensional equations of motion read

$$\begin{bmatrix} 1 & 0 \\ 0 & \nu \end{bmatrix} \begin{bmatrix} \xi'' \\ \zeta'' \end{bmatrix} + \begin{bmatrix} 0 & \kappa \\ -\kappa & 1 \end{bmatrix} \begin{bmatrix} \xi' \\ \zeta' \end{bmatrix} + \begin{bmatrix} 1 & 0 \\ 0 & 0 \end{bmatrix} \begin{bmatrix} \xi \\ \zeta \end{bmatrix} = \begin{bmatrix} f(\eta t) \\ 0 \end{bmatrix}. \tag{16}$$

The final mathematical model (Equation 16) contains only the two dimensionless parameters κ and ν. The coefficient κ can be interpreted as the strength of the coupling between the mechanical and the electrical system. It depends for example, on the remanent flux of the permanent magnet, the coil parameters and the geometric properties of the damping model. The parameter ν is the ratio of the mechanical eigenfrequency of the system and the electric time constant. Therefore, it can be seen as a relative self inductance and depends on the coil parameters – a value of $\nu = 0$ means, that the self inductance of the coil is neglected, whereas an increase of ν means, that the electric time constant increases, and therefore either the self inductance was increased or the resistance of the coil was reduced.

3.2 | Dynamic analysis of single DoF oscillator

Since the resulting equations of motion form a linear system, a dynamic analysis is straight forward. The frequency response functions for different parameters are found in Figures 4 and 5.

In Figure 4, the frequency responses of the single DoF oscillator are shown for different values of the electromagnetic coupling κ and a value of $\nu = 0$, and thus neglecting the inductance of the electric network. For $\kappa = 0$ the system is identical to an undamped oscillator. Increasing the coupling coefficient, the system behaves like a viscous damped oscillator. Critical damping occurs for $\kappa = \sqrt{2}$. If however, the inductance ν is raised, the frequency response differs, which is shown in Figure 5. Depending on the value of ν the resonance frequency shifts and in order to achieve the lowest maximum in the frequency response, an optimum exists. The different behavior can be explained by looking at the force-velocity-plot in Figure 6. For values of $\nu > 0$ the inductive damping element no longer behaves as an ideal viscous damper – which means, that the electromagnetic force is directly proportional to the velocity. Instead, the phase of the damping force shifts with respect to the velocity due to the electric time constant. This behavior was also found in ref. [1].

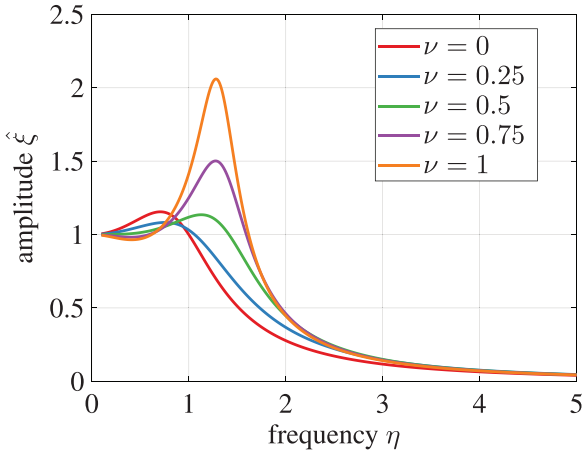

FIGURE 5 Frequency response function of single DoF Oscillator with inductive damping element for different values of ν and a value of $\kappa = 1$. DoF, degree of freedom.

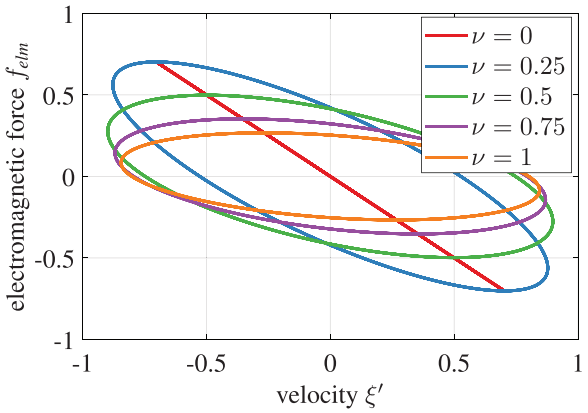

FIGURE 6 Damping force over velocity for different values of ν for an excitation frequency of $\eta = 3$ and $\kappa = 1$.

4 | CONCEPT OF INDUCTIVE MODE SELECTIVE DAMPING

To establish the concept of the mode selective damping, a three mass oscillator is investigated, see Figure 7. The oscillator chain features two inductive damping elements, which are attached between the masses. The inductive elements can be interconnected in different ways, which are shown in Figure 8.

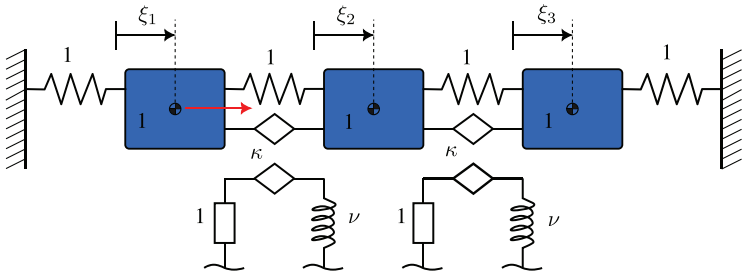

FIGURE 7 Oscillator chain with three masses and inductive damping elements.

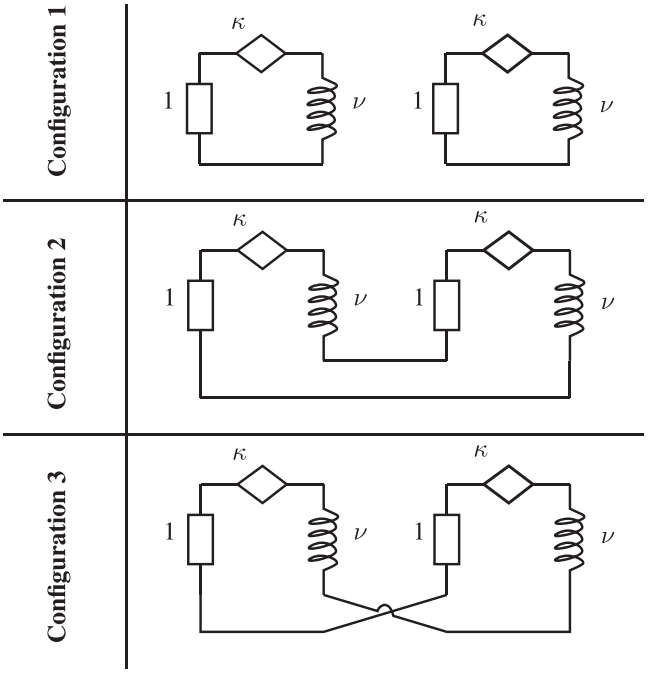

FIGURE 8 Overview of the different wiring options for the two inductive damping elements.

4.1 | Equations of motion of oscillator chain

Depending on the respective wiring of the inductive dampers, the equations of motion differ. Using the same abbreviations as for the single DoF oscillator, they read in non-dimensional form for the individual dampers (configuration 1)

$$\begin{bmatrix} 1 & 0 & 0 & 0 & 0 \\ 0 & 1 & 0 & 0 & 0 \\ 0 & 0 & 1 & 0 & 0 \\ 0 & 0 & 0 & \nu & 0 \\ 0 & 0 & 0 & 0 & \nu \end{bmatrix} \begin{bmatrix} \xi_1'' \\ \xi_2'' \\ \xi_3'' \\ \zeta_1'' \\ \zeta_2'' \end{bmatrix} + \begin{bmatrix} 0 & 0 & 0 & -\kappa & 0 \\ 0 & 0 & 0 & \kappa & -\kappa \\ 0 & 0 & 0 & 0 & \kappa \\ \kappa & -\kappa & 0 & 1 & 0 \\ 0 & \kappa & -\kappa & 0 & 1 \end{bmatrix} \begin{bmatrix} \xi_1' \\ \xi_1' \\ \xi_3 \\ \zeta_1' \\ \zeta_2 \end{bmatrix} + \begin{bmatrix} 2 & -1 & 0 & 0 & 0 \\ -1 & 2 & -1 & 0 & 0 \\ 0 & -1 & 2 & 0 & 0 \\ 0 & 0 & 0 & 0 & 0 \\ 0 & 0 & 0 & 0 & 0 \end{bmatrix} \begin{bmatrix} \xi_1 \\ \xi_2 \\ \xi_3 \\ \zeta_1 \\ \zeta_2 \end{bmatrix} = \begin{bmatrix} f(\eta\tau) \\ 0 \\ 0 \\ 0 \\ 0 \end{bmatrix}. \tag{17}$$

The system has three mechanical DoFs and two electrical DoFs. For the linking in series (configuration 2), the governing equations are given by

$$\begin{bmatrix} 1 & 0 & 0 & 0 \\ 0 & 1 & 0 & 0 \\ 0 & 0 & 1 & 0 \\ 0 & 0 & 0 & 2\nu \end{bmatrix} \begin{bmatrix} \xi_1'' \\ \xi_2'' \\ \xi_3'' \\ \zeta'' \end{bmatrix} + \begin{bmatrix} 0 & 0 & 0 & -\kappa \\ 0 & 0 & 0 & 0 \\ 0 & 0 & 0 & \kappa \\ \kappa & 0 & -\kappa & 2 \end{bmatrix} \begin{bmatrix} \xi_1' \\ \xi_1' \\ \xi_3 \\ \zeta' \end{bmatrix} + \begin{bmatrix} 2 & -1 & 0 & 0 \\ -1 & 2 & -1 & 0 \\ 0 & -1 & 2 & 0 \\ 0 & 0 & 0 & 0 \end{bmatrix} \begin{bmatrix} \xi_1 \\ \xi_2 \\ \xi_3 \\ \zeta \end{bmatrix} = \begin{bmatrix} f(\eta\tau) \\ 0 \\ 0 \\ 0 \end{bmatrix} \tag{18}$$

and for the linking in opposite phase (configuration 3), they read

$$\begin{bmatrix} 1 & 0 & 0 & 0 \\ 0 & 1 & 0 & 0 \\ 0 & 0 & 1 & 0 \\ 0 & 0 & 0 & 2\nu \end{bmatrix} \begin{bmatrix} \xi_1'' \\ \xi_2'' \\ \xi_3'' \\ \zeta'' \end{bmatrix} + \begin{bmatrix} 0 & 0 & 0 & -\kappa \\ 0 & 0 & 0 & 2\kappa \\ 0 & 0 & 0 & -\kappa \\ \kappa & -2\kappa & \kappa & 2 \end{bmatrix} \begin{bmatrix} \xi_1' \\ \xi_1' \\ \xi_3 \\ \zeta' \end{bmatrix} + \begin{bmatrix} 2 & -1 & 0 & 0 \\ -1 & 2 & -1 & 0 \\ 0 & -1 & 2 & 0 \\ 0 & 0 & 0 & 0 \end{bmatrix} \begin{bmatrix} \xi_1 \\ \xi_2 \\ \xi_3 \\ \zeta \end{bmatrix} = \begin{bmatrix} f(\eta\tau) \\ 0 \\ 0 \\ 0 \end{bmatrix}. \tag{19}$$

Since the two damping elements are linked, there is only one electric DoF for the configurations two and three, and thus the number of DoFs of the system reduces by one compared to configuration one.

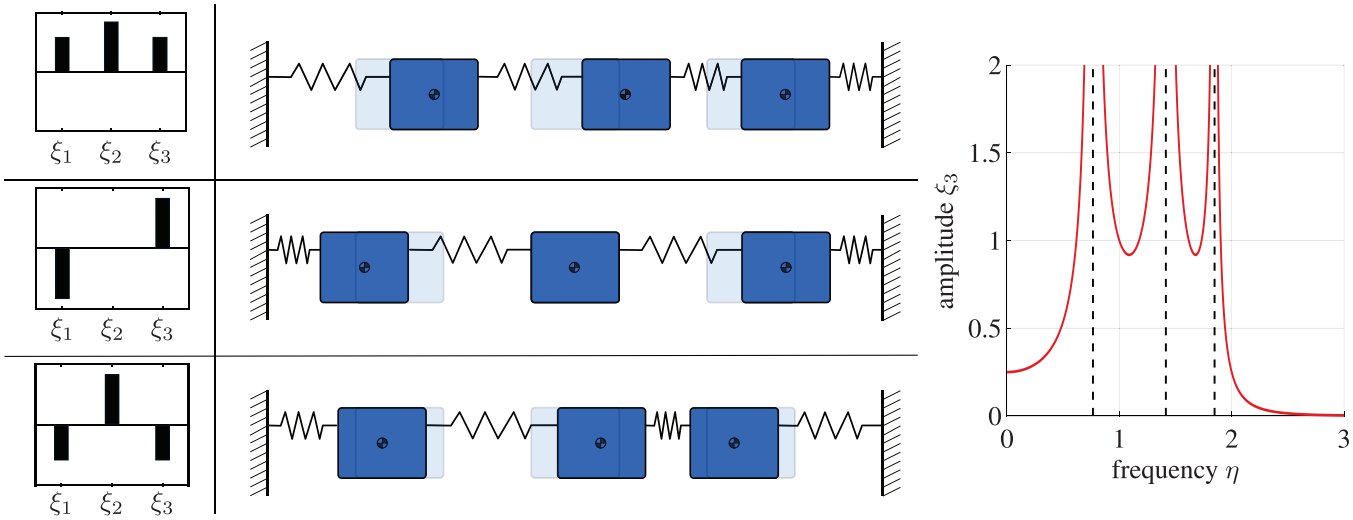

FIGURE 9 Modeshapes of the mechanical oscillator chain and frequency response of the third mass.

4.2 | Dynamic analysis of the oscillator chain with mode selective damping

To start the investigations the well known case of the undamped system is briefly discussed – this coincides with open electric circuits or no electromechanical coupling and thus $\kappa = 0$. In Figure 9, the mode shapes as well as the frequency response for the undamped scenario are shown.

In the first mode all three masses move together, but the middle mass has a slightly higher amplitude. In the second mode, the centered mass does not move at all, the adjacent masses move in opposite directions. And in the third mode, the centered mass moves in opposite direction to the outer masses. For all three modes, the change in length of the two electromagnetic damping elements is equal in magnitude, but the signs differ in the first and third mode. In the frequency response function of the third mass (see right hand side of Figure 9), three resonant frequencies occur.

For the three configurations shown in Figure 8 additional electrical DoFs exist and thus, the system has additional modes. But since the electric system on itself is not capable of vibrating, the electrical DoFs do not add any additional resonance frequencies to the system. Instead, the additional modes describe a transient decay as well as an arbitrary addition of charges in the electric domain – which can be interpreted as an analogy to a rigid body motion in the mechanical domain. Due to the symmetrical structure of the model, the characteristics of the mode shapes of the mechanical part are retained.

In Figure 10, the damping ratios of the different configurations i are compared for each mode j. For the results the electromagnetic coupling coefficient is set to $\kappa = 1$ and the inductance term is set to $\nu = 0.25$. For all configurations the

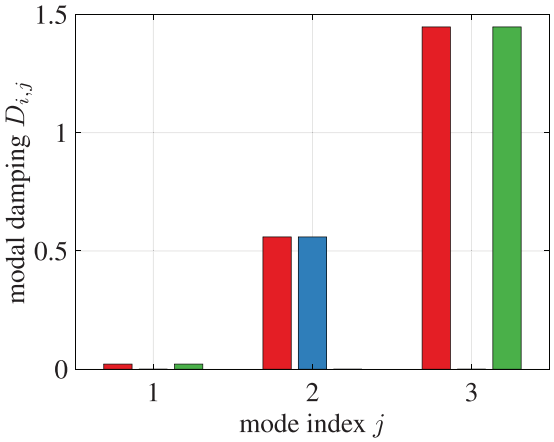

FIGURE 10 Comparison of the damping ratios for the different modes of the oscillator chain.

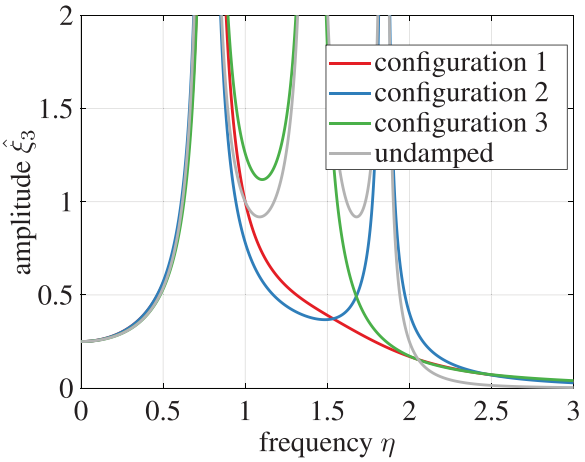

FIGURE 11 Frequency response of third mass for the different configurations as well as the undamped reference model.

first mode is almost undamped, since there is only little movement between the masses, as all masses move together – though the amplitudes of the centered mass are slightly higher. In the second configuration, the first mode is not damped at all, as the voltage induced in the first damper is opposite to the voltage induced in the second damper and therefore no current flows in this case. The second mode is damped only for the configurations one and two. In the third configuration no damping is obtained for this mode. While the induced voltages add up in the second configuration, they cancel each other out in the third configuration in this case. The third mode shows the opposite behavior. Here, in configuration two the induced voltages cancel each other out, while in configuration three they add up. The effect of the different configurations on the frequency response can be seen in Figure 11. While in configuration one, the second and the third mode are damped effectively, the configurations 2 and 3 only damp one of the modes and therefore, the system is capable of only damping specific modes.

5 | CONCLUSION

This paper provided a first look at the concept of an inductive mode selective damping system. Therefore, at first the dynamic behavior of the inductive damping element was illustrated by means of a single DoF oscillator. It could be shown, that the damper acts as an ideal viscous damper only if the inductance of the coil is negligible. Otherwise, the electrical system has its own dynamic, which leads to a phase shift, of the electromagnetic force and the velocity. Through implementing two of such damping elements in an oscillator chain and varying the wiring configurations, it was observed, that the damping characteristics altered. The damping of specific modes could individually be switched on and of by changing the wiring of the damping elements. Since the change between the different configurations requires only adjustments in the electrical domain, it can be done easily – even during operation – because only switches have to be flipped. In this work, the method has only been applicated to a symmetric model, where the displacements of the masses in different modes are equal in magnitude. In future research, the method will also be applicated to asymmteric models. It is assumed, that the concept of mode selective damping will also perform well in this scenario, provided that the coil parameters, such as the number of turns, are appropriately adapted.

ACKNOWLEDGMENTS

Open access funding enabled and organized by Projekt DEAL.

ORCID

Mitja Rosenboom https://orcid.org/0000-0001-6640-5412

REFERENCES

1. Palomera-Arias, R. (2005). *Passive electromagnetic damping device for motion control of building structures* [Doctoral Thesis]. Massachusetts Institute of Technology.

2. Laborenz, J., Siewert, C., Panning, L., Wallaschek, J., Gerber, C., & Masserey, P. A. (2010). Eddy current damping: A concept study for steam turbine blading. *Journal of Engineering for Gas Turbines and Power*, *132*, 052505.
3. Bae, J. S., Kwak, M. K., & Inman, D. J. (2005). Vibration suppression of a cantilever beam using eddy current damper. *Journal of Sound and Vibration*, *284*(3-5), 805–824.
4. Palomera-Arias, R., Connor, J. J., & Ochsendorf, J. (2008). Feasibility study of passive electromagnetic damping systems. *Journal of Structural Engineering*, *134*(1), 164–170.
5. Zhu, X., Jing, X., & Cheng, L. (2012). Magnetorhelogical fluid dampers: A review on structure design and analyses. *Journal of Intelligent Material Systems and Structures*, *23*, 839–873.
6. Alhams, A., Qazak, A., Badri, Y., Sassi, S., Renno, J. M., & Sassi, A. (2024). Design and testing of a hybrid electromagnetic damping device for automotive applications. *Journal of Magnetism and Magnetic Materials*, *589*, 171606.
7. Crandall, S. H. (2017). *Dynamics of mechanical and electromechanical systems*. MedTech.

How to cite this article: Rosenboom, M., & Hetzler, H. (2024). Inductive mode selective damping of structural vibrations. *Proceedings in Applied Mathematics and Mechanics*, *24*, e202400212.
https://doi.org/10.1002/pamm.202400212